Geodetic measurements of convergence across the New Hebrides subduction zone

Stéphane Calmant[1], Pierre Lebellegard[1], Fred Taylor[2], Michael Bevis[3], Didier Maillard[4], Jacques Récy[5], and Jocelyne Bonneau[1]

Abstract. Between 1990 and 1994, geodetic measurements (GPS observations) have been conducted across the New Hebrides subduction zone where the Australia plate subducts under the New Hebrides Arc. This paper establishes convergence rate variations along the trench. In the South, at Tanna, the relative motion is oriented N244 ± 4 and has a uniform rate of 11.7 ± 0.8 cm/yr. The rate at Efaté is 10.3 ± 0.9 cm/yr, oriented N242 ± 4. Both azimuths very well compare with slip vectors of the last major earthquakes. In the North, the rate at Santo is only 3.6 ± 1.2 cm/yr, oriented N253 ± 26. The difference in the convergence rates between Santo on the one hand and Efaté and Tanna in the other hand points to a right lateral shear zone between Santo and Efaté. At Santo where the plate coupling is very high, the very low convergence rate might be related to the absence of recent strong earthquakes. No significant variations are detected for the baselines within the Australia plate.

Introduction

The New Hebrides subduction zone is part of the convergent plate boundary between the Australia and Pacific plates (Figure 1). Along this trench, the Australia plate subducts eastward under the New Hebrides Arc which borders the North Fiji Basin created by back arc spreading. Taking advantage of the presence of islands at close distances on both sides of the trench (baselines across the trench extend from 252 km to 580 km in length), we conducted GPS measurements in order to determine the convergence rate across the trench. We performed observations at sites on Lifou and Maré Islands on the Loyalty Ridge, at Nouméa on the island of New Caledonia, and at sites on the islands of Santo, Efaté and Tanna, in the southern half of the New Hebrides Arc (Figure 1). Tanna and Efaté belong to the peri-Pacific volcanic belt, while Santo is a piece of the inner subduction wall uplifted by the subduction of the facing d'Entrecasteaux Ridge [*Taylor et al.*, 1980].

The GPS data

GPS data were produced during campaigns conducted from 1990 to 1994. In 1990 and 1992, the GPS campaigns were those of the US South West Pacific Project [*Schutz et al.*, 1993]. The other campaigns were conducted by the ORSTOM Laboratory of Geophysics in Nouméa (see list in Table 1). Data were processed with version 3.4 of the Bernese GPS software [*Rothacher et al.*, 1993]. The precise ephemerides distributed by the IGS center CODE (University of Bern) were used. Site positions were computed in single baseline mode, using the site of Lifou as a fixed reference site, and a no fiducial approach. All the site coordinates given further on refer to this fixed point on the Australia plate. The GPS results are given as weighted least square epoch averages computed from the daily solutions. The weights were computed on the basis of the formal errors, scaled in order that the reduced χ^2 factor equals 1 [*Dixon et al.*, 1991; *Larson and Agnew*, 1991] for each epoch. The uncertainties reported for these epoch solutions are twice the a-posteriori uncertainties.

We divided the geodetic net into two subnets: the New Hebrides subnet which includes Santo, Efaté, Tanna and Lifou, and the New Caledonia subnet, including Nouméa, Maré and Lifou. Within the New Hebrides subnet, the different motions relative to Lifou provide the spatial variation of the convergence rate across the trench, and relative motions between sites within the New Hebrides Arc would suggest
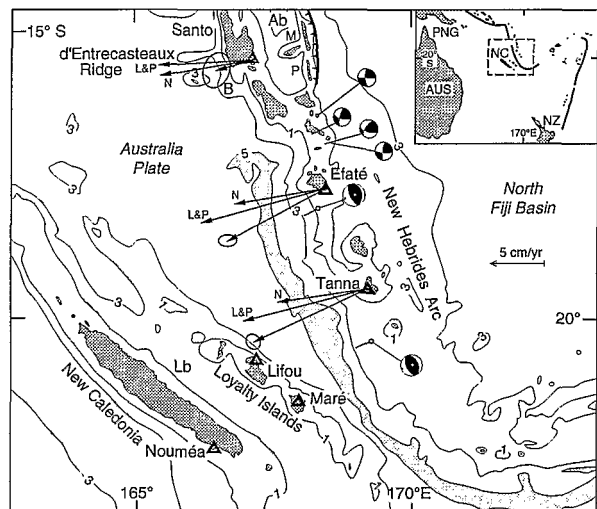
Figure 1: Situation map. Ab, Aoba basin; M, Maewo island; P, Pentecost island; B, Bougainville guyot; Lb, Loyalty basin. Triangles mark the location of the GPS sites. Vectors show relative plate motion from this study (tipped with ellipses), for NUVEL-1 (label N) and Louat & Pelletier (label L&P). CMT solutions and slip vector azimuth for the last thrust-type earthquakes are shown. CMT solutions of strike-slip events between Santo and Efaté are also given. In upper right icon, PNG, Papua New Guinea; NC, New Caledonia; AUS, Autralia; NZ, New Zealand.

[1] Laboratoire de Géologie-Géophysique, Centre ORSTOM de Nouméa, Nouvelle-Calédonie
[2] University of Texas at Austin, U S A
[3] Hawaii Institute of Geophysics, U S A
[4] Institut Géographique National, Paris, France
[5] Laboratoire de Géologie-Géophysique, Centre ORSTOM de Villefranche sur Mer, France

Table 1. Design of the GPS campaigns and site occupations

Epoch	Receiver	rate * (sec)	Sessions (days in year)	L M N T E S
08 / 90	Trimble 4000SST	15	local night (214 to 219)	X X X X X X
08 / 92	Trimble 4000SST	15	2 x 10 h / day (212 to 219)	X X X X X X
10 / 92	Leica/Wild SR299	30	20 h / day (300 to 302)	X X
01 / 93	Leica/Wild SR299	30	22 h / day (18 to 24)	X X X X X
06 / 93	Ashtech LX II	30	22 h / day (178 to 183)	X X X X
11 / 93	Leica/Wild SR299	30	22 h / day (327 to 330)	X X X X X
12 / 93	Leica/Wild SR299	30	22 h / day (333 to 338)	X X
03 / 94	Leica/Wild SR299	30	22 h / day (79 to 83)	X X X
07 / 94	Leica/Wild SR299	30	22 h / day (186 to 190)	X X X

L: Lifou, M: Maré, N: Nouméa, T: Tanna, E: Efaté, S: Santo
* Data were processed at the same rate that they were collected.

intra-arc deformation. Within the New Caledonia subnet, any motion relative to Lifou would suggest internal plate deformations.

Results

The successive GPS measurements obtained for the sites of the New Hebrides subnet are reported in Figures 2 (plane series) and 3 (time series). It is worthwhile to note that in the time series the best fitting trends result of least square adjustments weighted by means of the complete posterior covariance matrices of the epoch averages. The rates of displacement with time are also given at twice the posterior uncertainties. Tanna is the southernmost site within the New Hebrides Arc, and the one of the subnet for which the baseline across the trench to Lifou (252 km) is shortest. The plane series shows a precise N244 ± 4 trend in the positions. When fitted versus time in the hypothesis of uniform motion, these positions indicate a relative motion of 11.7 ± 0.8 cm/yr. The site of Efaté occupies an intermediate location in the subnet. The baseline length with Lifou is 360 km. The relative positions for this site in the plane series are more scattered along the southwestward trend than those for Tanna. The best fitting orientation for the trend is N242 ± 4 and the rate along this trend is 10.3 ± 0.9 cm/yr. Santo is the northernmost site studied. It is connected with Lifou by a 580 km long baseline, the longest one in the net. Since the raw data for epoch 08/90 were not available, we have used the position given by *Schutz et al.* [1993]. This value, given in absolute position, had to be translated to our local system. We have used the absolute (ITRF) coordinates of the DORIS beacon at Nouméa to tie both systems. The 2σ ellipse associated with this position accounts for the repeatabilities given by *Schutz et al.* [1993], the repeatabilities of the tie between the GPS site and the DORIS beacon at Nouméa and 5 cm (on each coordinate) stated for the uncertainty on the location of the DORIS beacon. The best fitting rate of Santo is 3.6 ± 1.2 cm/yr, oriented N253 ± 26. The azimuth of the relative motion for this site is weakly

constrained because of the large data uncertainties relative to the magnitude of the rate.

The different positions obtained for the sites of Maré and Nouméa, in the New Caledonia subnet, are given in Figures 4 (plane series) and 5 (time series). The Maré-Lifou and Nouméa-Lifou baselines are the shortest resolved baselines, measuring respectively 114 and 182 km. On the plane series, the observed positions for each site lie within ± 1 milli arc-second around an average position, and no trends develop clearly. Nevertheless, when fitted versus time, these series give relative motions of 1.4 ± 0.7 cm/yr oriented N222 ± 24 for Nouméa and 1.6 ± 0.7 cm/yr oriented N135 ± 18 for Maré. However, these 2-parameter fits (uniform motions) have larger χ^2 and weighted rms than the 1-parameter fits (no motion). The no relative motion result is thus retained for both sites.

Discussion

By using focal mechanisms, magnetic anomalies and the global plate model RM2 of *Minster and Jordan* [1978], *Louat and Pelletier* [1989, further on L&P] have determined rates of convergence along the New Hebrides subduction zone (Table 2). They found that the convergence rate decreases from north to south from 15 cm/yr oriented N252 at 13°S, north of Santo, to 12 cm/yr oriented N255 at 20°S, i.e. between Santo and 22°S; but with a lower rate in front of Santo, where the d'Entrecasteaux Ridge collides with the trench leading to the uplift of that island. From the geometry of the lithospheric bulge associated to the subduction, *Dubois et al.* [1977] found a subduction rate of 12.4 cm/yr around 20°S. Finally, *Taylor et al.* [1994] determined an average convergence rate of 13.2
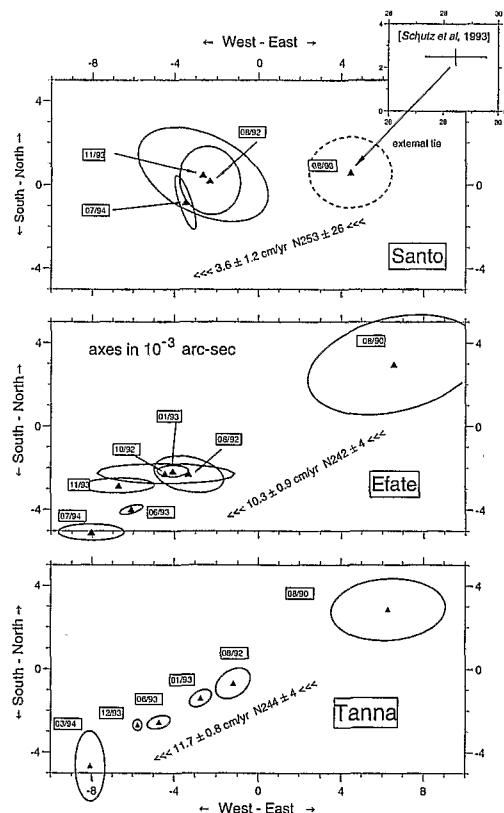
Figure 2: Plane series of GPS positions for sites on the New Hebrides islands. Triangles show epoch average of daily solutions. Ellipses are 2σ uncertainties.

and 3.6 cm/yr oriented N190 for Efaté, consistently with an almost North-South opening along the complex structure trending WNW-ESE in the north of the North Fiji Basin [*Louat and Pelletier*, 1989].

As far as the site on Santo is concerned, the convergence rate derived from the GPS results is much lower than the rates given by L&P and NUVEL-1 and the even larger value given by *Taylor et al.* [1994]. *Taylor et al.* [1987 and 1990] have shown that at Santo, where plate coupling is high [*Louat et al.*, 1988], up to one third of the slip may be related to the recurrent strong seismic events. Part of the discrepancy between observed and expected rates may thus be due to the absence of such strong seismic events since 1965 [*Taylor et al.*, 1990], since the GPS-derived vector has been obtained during a period free of noticeable seismic event. Besides, *Louat et al.* [1988] showed that increased interplate coupling adjacent to the d'Entrecasteaux Ridge should result in a slow down of the convergence in that part of the trench. Thus, a permanent deformation within the arc and some back-arc compression might account for the rest of the discrepancy. *Collot et al.* [1985] report compression along the eastern side of the Central New Hebrides Arc. *Daniel et al.* [1989] report folds and faults consistent with a N086 compressive tectonic stress in the Aoba basin, an intra-arc basin east of Santo (Figure 1). Thrusting along the eastern border of the islands of Maewo and Pentecost is evidenced both on seismic grounds [*Louat and Pelletier*, 1989] and on tectonic grounds [*Collot et al.*, 1985].

To account for the differential motion between Santo and the southern sites, the New Hebrides Arc must undergo internal deformation. CMT solutions of the major events of a seismic crisis which occured in 1990 and which outline a right-lateral shear zone north of Efaté are reported in Figure 1. The area north of Efaté has long been recognized as one where the arc undergoes major structural changes, and *Collot et al.* [1985] report right lateral slip lines north and south of the collision zone.

The baselines within the New Caledonia subnet are stable all through the observation period. Thus, no strain accumulation within the subducting Australia plate is detected either trenchward along the Loyalty Ridge with the Lifou-Maré baseline, or backward within the Loyalty basin with the Lifou-Nouméa baseline. If strain accumulation is present in the subducting plate, we failed to detect it, as did *Larson and Lisowski* [1994] at the Pacific-Alaska convergence zone.

Conclusion

Spatial variations in the convergence rate along the New Hebrides trench are evidenced by repeated GPS observations of a net comprising sites on either side of the trench. The New Hebrides Arc which borders the overriding plate along the trench appears as a soft domain which undergoes most of the deformation due to the tectonic elements which disturb the subduction process.
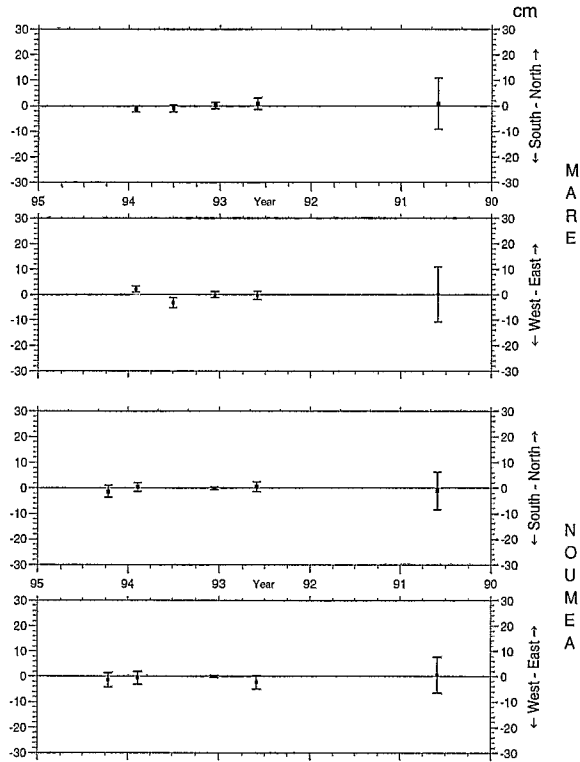
References

Collot, J. Y., J. Daniel, and R. V. Burne, Recent tectonics associated with the subduction/collision of the d'Entrecasteaux zone in the Central New Hebrides, *Tectonophysics, 112*, 325-356, 1985.

Daniel, J., M. Gerard, A. Mauffret, and scientific party, Déformation compressive d'un bassin intra-arc dans un contexte de collision ride-arc: le bassin d'Aoba, arc des Nouvelles-Hébrides, *C. R. Acad. Sci. Paris, 308*, Ser. II, 239-245, 1989.

DeMets, C, R. G. Gordon, D. F. Argus, and S. Stein, Current plate motions, *Geophys. J. Int., 101*, 425-478, 1990.

Dixon, T. H., G. Gonzalez, S. M. Lichten, and E. Katsigris, First epoch geodetic measurements with the global positioning system across the northern Caribbean plate boundary zone, *J. Geophys. Res., 96*, 2397-2415, 1991.

Dubois, J., J. Launay, J. Récy, and J. Marshall, New Hebrides trench: subduction rate from associated lithospheric bulge, *Canadian J. of Earth Sc., 14-2*, 250-255, 1977.

Dziewonski, A. M., G. Ekström, J. H. Woodhouse, and G. Zwart, Centroid-moment tensor solutions for January-March 1990, *Phys. Earth Planet. Int., 65*, 197-206, 1991.

Dziewonski, A. M., G. Ekström, and M. P. Salgnanik, Centroid-moment tensor solutions for January-March 1994, *Phys. Earth Planet. Int., 86*, 253-261, 1994.

Larson, K., and D.C. Agnew, Application of the global positioning system to crustal deformation measurement. 1. Precision and accuracy, *J. Geophys. Res., 96*, 16547-16565, 1991.

Larson, K., and M. Lisowski, Strain Accumulation in the Shumagin Islands: Results of initial GPS measurements, *Geophys. Res. Lett., 21*, 489-492, 1994.

Louat, R., M. Hamburger, and M. Monzier, Shallow and intermediate-depth seismicity in the New Hebrides arc: Constraints on the subduction process, in *Geology and off-shore resources of Pacific island arcs-Vanuatu region, Circum Pacific Council for Energy and Mineral Resources Earth Sciences Series, vol 8*, edited by H. Greene and F. Wong, pp. 329-355, Houston, Texas, 1988.

Louat, R., and B. Pelletier, Seismotectonics and present-day relative plate motions in the New Hebrides - North Fiji Basin region, *Tectonophysics, 167*, 41-55, 1989.

Minster, J. B., and Jordan T. H., Present-day plate motions, *J. Geophys. Res., 83*, 5331-5354, 1978.

Rothacher, M., G. Beutler, W. Gurtner, E. Brockman, and L. Nervart, *Documentation for Bernese GPS Software version 3.4*, Univ. Bern, 1993.

Schutz, B., M. Bevis, F. Taylor, D. Kuang, P. Abusali, M. Watkins, J. Recy, B. Perin, and O. Peyroux, The Southwest Pacific GPS Project: Geodetic results from Burst 1 of the 1990 field campaign, *Bull. Géodésique, 67*, 224-240, 1993.

Taylor, F. W., B. L. Isacks, C. Jouannic, A. L. Bloom, and J. Dubois, Coseismic and Quaternary vertical tectonic movements, Santo and Malekula islands, New Hebrides island arc, *J. Geophys. Res., 85*, 5367-5381, 1980.

Taylor, F. W., C. Frohlich, J. Lecolle, and M. Strecker, Analysis of partially emerged corals and reef terraces in the Central Vanuatu Arc: Comparison of contemporary coseismic and nonseismic with Quaternary vertical movements, *J. Geophys. Res., 92* , 4905-4933, 1987.

Taylor, F. W., R. L. Edwards, G. J. Wasserburg, and C. Frohlich, Seismic recurrence intervals and timing of aseismic subduction inferred from emerged corals and reefs of the Central Vanuatu (New Hebrides) frontal arc, *J. Geophys. Res., 95*, 393-408, 1990.

Taylor, F. W., T. M. Quinn, C. G. Gallup, and R. L. Edwards, Quaternary Plate Convergence Rates at the New Hebrides Island Arc from the Chronostratigraphy of Bougainville Guyot (Site 831), in *Proc. ODP, Sci Results, 134*, edited by H.G. Grenne, J.Y. Collot, L.B. Stokking et al., pp. 47-57, College Station, TX (Ocean Drilling Program), 1994.

S. Calmant, P. Lebellegard, and J. Bonneau, Centre ORSTOM, Nouméa Cedex, Nouvelle-Calédonie, (calmant@noumea.orstom.nc)

F. Taylor, Institute for Geophysics, University of Texas at Austin, Austin, TX, USA

M. Bevis, Hawaii Institute of Geophysics and Planetology, University of Hawaii, Honolulu, HI, USA

D. Maillard, IGN, Rue Pasteur, St Mandé, France
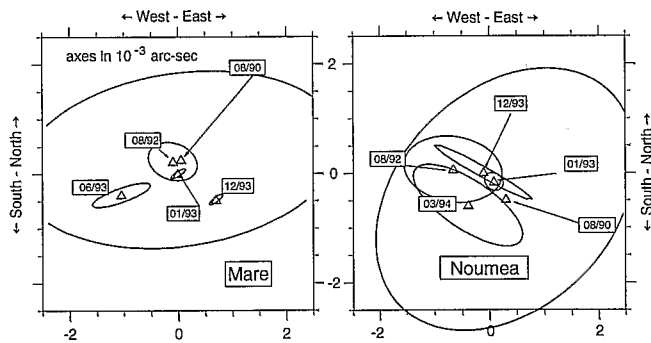
J. Récy, ORSTOM, B.P. 48, Villefranche s/mer, France
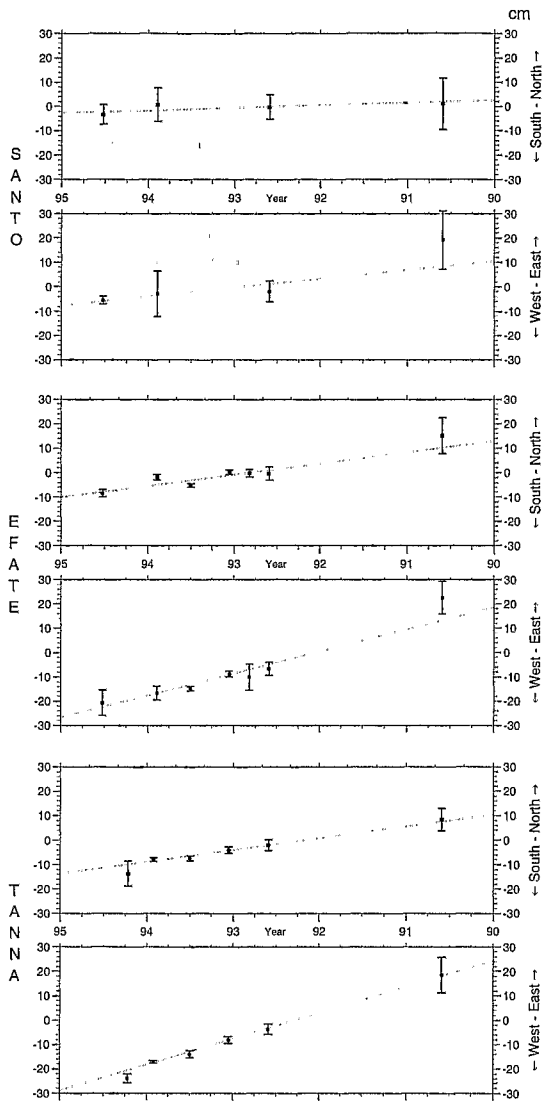
Figure 3: Time series for sites on the New Hebrides islands. Filled squares stand for the epoch average of daily solutions. Bars are 2σ uncertainties. Dotted line is best fitting time-dependent regression.

Figure 4: Plane series for sites on the Australia plate. Triangles show epoch average of daily solutions. Ellipses are 2σ uncertainties. Figures are centered on the all epoch average of all epoch solutions.

Figure 5: Time series for sites on the Australia plate. Filled squares stand for epoch average of daily solutions. Bars are 2σ uncertainties. 0 lines stand for the according coordinate of the best fitting time-independent regression.

± 1 cm/yr since 0.4 m.y. from the chronostratigraphy of Bougainville guyot, currently subducting south of Santo (Figure 1). The convergence vectors given by L&P and those given by NUVEL-1 [*DeMets et al.*, 1990] for the relative motion of Australia and Pacific plates are shown in Figure 1 together with the relative motions derived in the present study. The azimuths of the GPS-derived vectors at Tanna and Efaté coincide with that of the slip vectors deduced from the Centroid-moment tensor (CMT) solutions of the last major thrust-type earthquakes which recently occured south of Tanna (12 February 1994, M_S=7.1, slip oriented N244; *Dziewonski et al.* [1994]) and south of Efaté (5 March 1990, M_S = 7.0, slip oriented N243; *Dziewonski et al.* [1991]). Global models such as RM2 or NUVEL-1 do not take the back arc tectonics in the North Fiji Basin into account. If NUVEL-1, although poorly constrained in the Southwest Pacific, is taken as representative of the motion between the Australia and Pacific plates, the difference between NUVEL-1 and GPS-derived vectors is due to the crustal motion in the back arc area and in the North Fiji Basin. It is 4.5 cm/yr oriented N237 for Tanna

Table 2. Convergence vectors (cm/yr)

	Santo		Efaté		Tanna	
NUVEL-1	8.9	N260	8.6	N261	8.3	N261
L&P	9	N266			12	N255
This study	3.6±1.2 N253±26		10.3±0.9 N24±4		11.7±0.8 N244±4	